Chemistry & Biology
Article

Loop Grafting of *Bacillus subtilis* Lipase A: Inversion of Enantioselectivity

Ykelien L. Boersma,[1] Tjaard Pijning,[2] Margriet S. Bosma,[1] Almer M. van der Sloot,[3] Luís F. Godinho,[1] Melloney J. Dröge,[4] Remko T. Winter,[1] Gertie van Pouderoyen,[2] Bauke W. Dijkstra,[2] and Wim J. Quax[1,*]
[1]Department of Pharmaceutical Biology, Groningen University Institute for Drug Exploration (GUIDE), University of Groningen, A. Deusinglaan 1, 9713 AV Groningen, The Netherlands
[2]Laboratory of Biophysical Chemistry, University of Groningen, Nijenborgh 4, 9747 AG Groningen, The Netherlands
[3]Department of Systems Biology, CRG-EMBL, Dr. Aiguader 88, 08003 Barcelona, Spain
[4]ABL BV, Postbus 232, 9400 AE Assen, The Netherlands
*Correspondence: w.j.quax@rug.nl
DOI 10.1016/j.chembiol.2008.06.009

SUMMARY

Lipases are successfully applied in enantioselective biocatalysis. Most lipases contain a lid domain controlling access to the active site, but *Bacillus subtilis* Lipase A (LipA) is a notable exception: its active site is solvent exposed. To improve the enantioselectivity of LipA in the kinetic resolution of 1,2-O-isopropylidene-*sn*-glycerol (IPG) esters, we replaced a loop near the active-site entrance by longer loops originating from *Fusarium solani* cutinase and *Penicillium purpurogenum* acetylxylan esterase, thereby aiming to increase the interaction surface for the substrate. The resulting loop hybrids showed enantioselectivities inverted toward the desired enantiomer of IPG. The acetylxylan esterase-derived variant showed an inversion in enantiomeric excess (*ee*) from −12.9% to +6.0%, whereas the cutinase-derived variant was improved to an *ee* of +26.5%. The enantioselectivity of the cutinase-derived variant was further improved by directed evolution to an *ee* of +57.4%.

INTRODUCTION

Stricter regulations of the US Food and Drug Administration (FDA) have imposed the use of enantiopure pharmaceuticals (Blaser et al., 2005; Breuer et al., 2005), which has led to an increased demand of the chemical industry for enantioselective catalysts. Enzymes can offer the necessary high enantioselectivity combined with efficient catalysis and few by-products (Schmid et al., 2001; Zhao et al., 2002). A prime example of a successful application of an enzyme in enantioselective biocatalysis is provided by lipases. These enzymes are active in both aqueous and low-water media, and they can convert a large variety of (synthetic) molecules. The most common application of lipases is in the preparation of chiral building blocks, especially by kinetic resolution of racemic mixtures (Beisson et al., 2000). To understand the molecular details of catalysis by lipases, 3D structures of 38 different lipases have been elucidated. All structures show an α/β-hydrolase fold, with the catalytic serine located at the so-called nucleophile elbow (Beisson et al., 2000; Holmquist, 2000), and the other two catalytic triad residues, Asp and His, in close proximity. Most lipases contain a lid domain controlling access to the active site (Eggert et al., 2004). The interaction of the enzyme with lipid aggregates induces the displacement of the lid, which makes the active site accessible to individual substrate molecules and increases the catalytic activity. This phenomenon is known as interfacial activation. The amino acid composition of the lid has been shown to affect both the specificity as well as the enantioselectivity of lipases (Beisson et al., 2000; Secundo et al., 2004; Verger, 1997).

The *Bacillus subtilis* 168 Lipase A (LipA) is of particular interest, since it does not show interfacial activation. In agreement with this, it has been found that it does not contain a lid, and that its active site is solvent exposed (Van Pouderoyen et al., 2001). Due to its small size and relatively low molecular mass (181 amino acid residues, 19 kDa), the *B. subtilis* LipA can be regarded as a minimal α/β-hydrolase fold enzyme (Dartois et al., 1992, 1994; Dröge et al., 2006; Lesuisse et al., 1993; Van Pouderoyen et al., 2001). Other small α/β-hydrolase fold esterases without a lid include the 21 kDa cutinase from *Fusarium solani* (197 amino acid residues; PDB entry 1CEX [Longhi et al., 1997; Martinez et al., 1992]) and the 22 kDa acetylxylan esterase (AXE) from *Penicillium purpurogenum* (207 residues; PDB entry 1G66 [Ghosh et al., 1999]). Their 3D structures are similar to that of LipA, with five parallel β strands and four α helices, and their active sites are also solvent exposed. However, the substrate-binding cleft of LipA is shallower and wider than those of 1CEX and AXE; the loops lining the cleft of LipA are shorter and do not extend as much from the core of the protein as in 1CEX and AXE (Van Pouderoyen et al., 2001).

In this study, we investigated the effect on the activity and enantioselectivity of LipA of replacing a short active-site-lining loop by the longer loops from 1CEX and AXE, thereby extending this loop by three or two amino acids, respectively. It was shown previously that this active-site-lining loop is of key importance to the enantioselectivity of LipA (Dröge et al., 2006). We hypothesized that this replacement could increase the interaction surface with the substrate and affect its enantioselectivity. Indeed, we found that the loop replacement yielded LipA variants with improved enantioselectivity. The AXE-derived variant showed a change in enantiomeric excess (*ee*) from −12.9% to +6.0%, whereas the cutinase-derived variant was improved to an *ee* of +26.5%. The enantioselectivity of the cutinase-derived variant

could be further improved by directed evolution to an *ee* of +57.4%.

RESULTS

Modeling of the Loop Mutants

B. subtilis LipA, as well as *F. solani* cutinase (1CEX) and *P. purpurogenum* acetylxylan esterase (AXE), can be regarded as a minimal α/β-hydrolase fold enzyme, as it is lacking a lid domain. LipA shares 14% homology with 1CEX (Q-score of 0.29, SSM server http://www.ebi.ac.uk/msd-srv/ssm [Krissinel and Henrick, 2005]) as well as with AXE (Q-score of 0.28). The 3D structure of *B. subtilis* LipA is similar to those of 1CEX and *P. purpurogenum* AXE, superimposing with rmsd values of 1.9 Å and 2.9 Å, respectively (Van Pouderoyen et al., 2001) (Figure 1A). Several residues of the loop from residue 12 to residue 21 line the hydrophobic pocket that holds the IPG moiety of the IPG phosphonate inhibitors covalently bound to LipA (Dröge et al., 2006). Among these residues, N18 has been previously suggested to be important for the enantioselective properties of LipA (Dröge et al., 2006; Van Pouderoyen et al., 2001). Therefore, residues 12–20 were chosen for exchange with the corresponding loop from cutinase (residues 42–53). Modeling this longer loop in the LipA 3D structure by using the SWISS-MODEL server (http://swissmodel.expasy.org [Arnold et al., 2006]) (Figures 1B and 1C) suggests that the first β strand in LipA, which runs from residue 3 to residue 11, is elongated with a Ser and a Thr at positions 12 and 13, respectively, after which the peptide chain makes a turn at a E14 and, via T15, returns to a G16, which occupies a position equivalent to G13 in the parent LipA molecule. In this way, a larger binding surface is created for IPG with residues that may interact with IPG, which are S12, T13, N17 and L21, and E14 and T15.

Residues 11–21 were chosen for exchange with the corresponding loop from AXE (residues 12–23). From the SWISS-MODEL-generated structure, shown in Figures 1D and 1E, it can be seen that the first β strand (residues 3–11 in LipA) is again elongated by two residues, now E11 and T12. The loop makes a turn at T13 and returns to S15 (equivalent to G13 in LipA) via A14. Here, residues that may interact with IPG are E11, T12, A14, and S20.

Characterization of the Loops

The LipA wild-type loop was replaced by the two loops described above. The resulting constructs were sequenced to verify their nucleotide sequences, which were found to be correct. From SDS-PAGE analysis, it was seen that the loop hybrids were translocated to the periplasmic space (Figure 2). The expression of the loop hybrids was found to be comparable to that of wild-type LipA. A first screen on activity by using *p*-nitrophenyl caprylate showed a conversion to the yellow *p*-nitrophenol by both loop variants. The activity and enantioselectivity in the conversion of IPG butyrate is given in Table 1. The activity was found to be comparable to that of wild-type LipA, with conversions of 20.9% and 29.7% for the AXE and 1CEX loop variants, respectively, versus 28.2% for wild-type LipA. However, compared to the wild-type enzyme (*ee* of −12.9%) the enantioselectivity of the variants was inverted toward the desired enantiomer of IPG. The AXE variant showed a slight improvement in *ee* to +6.0%, whereas the cutinase-derived variant was improved to an *ee* of +26.5%. Interestingly, the cutinase wild-type enzyme also showed an enantiopreference toward *S*-(+)-IPG, with an *ee* of +40.5% (Table 1). The K_M value of the 1CEX-derived variant toward *S*-(+)-IPG was not significantly lowered compared to the wild-type (Table 2). The 1CEX hybrid appeared to be the more promising variant in terms of enantioselectivity. Since the models showed that L21 may interact with IPG, and that L21 is in a position equivalent to that of N18 in wild-type LipA, a residue that has been shown to be important for the enzyme's enantioselectivity (Dröge et al., 2006; Eggert et al., 2005), L21 was selected for saturation mutagenesis and subsequent selection.

Directed Evolution of the 1CEX Loop

After the transformation of *Escherichia coli* HB2151, a mutant library on position L21 consisting of 1250 clones was obtained. Sequence analysis of ten clones revealed that one clone had no mutation at position 21 and that two clones had a mutation to serine, whereas the other seven clones all had a different amino acid mutation. Considering its size of 1250 clones and the use of a NNS codon, the library was found to have sufficient variability at position 21.

The library was subjected to the growth-selection assay, based on an aspartate auxotrophy (Boersma et al., 2008). Minimal medium was supplemented with enantiopure IPG coupled to aspartate, whereas selection pressure was increased by the addition of an enantiopure IPG phosphonate. All selected mutants showed a further improvement of the inverted enantioselectivity from an *ee* of +26.4% to an *ee* of +57.4% for the best variant, L21Q (Figure 3). Selection was in favor of mutation L21G, which was observed six times. Remarkably, the parent 1CEX sequence was not retrieved. Together with the L21Q mutation, which was observed three times, the L21G mutant showed an activity toward the IPG ester comparable to that of the parent loop mutant (29.7% for the parent loop mutant versus 22.4% and 28.3% for L21G and L21Q, respectively). As these mutations had an advantageous effect on the enantioselectivity, as reflected in an improved *ee* value, the L21G and L21Q mutants were further characterized. The expression of the 1CEX parent variant and mutants L21G and L21Q in the periplasm was found to be comparable (Figure 2). All three had a lowered affinity toward *S*-(+)-IPG, although this value was not significant ($p > 0.05$; Table 2).

Due to their frequency of retrieval and their enantioselectivity, L21G and L21Q were used to parent a second mutant library at position T20. According to the model, residue T20 was unlikely to interact with IPG, in contrast to residue L21. Hence, no effect on the enzyme's enantioselectivity was expected upon mutagenesis of T20. After transformation of *E. coli* HB2151, two mutant libraries consisting of 1000 clones were obtained. Sequence analysis of ten clones from each library revealed that all variants showed a different mutation. Thus, the libraries were found to be satisfactory. Then, both libraries were used in the growth-selection assay, colonies were picked, the periplasm was isolated, and the activity and enantioselectivity toward racemic IPG butyrate was determined (Figure 4). The highest improvement in *ee* was observed for variant T20K/L21G, from an *ee* of +31.7% to an *ee* of +67.7%. However, most variants showed a significant

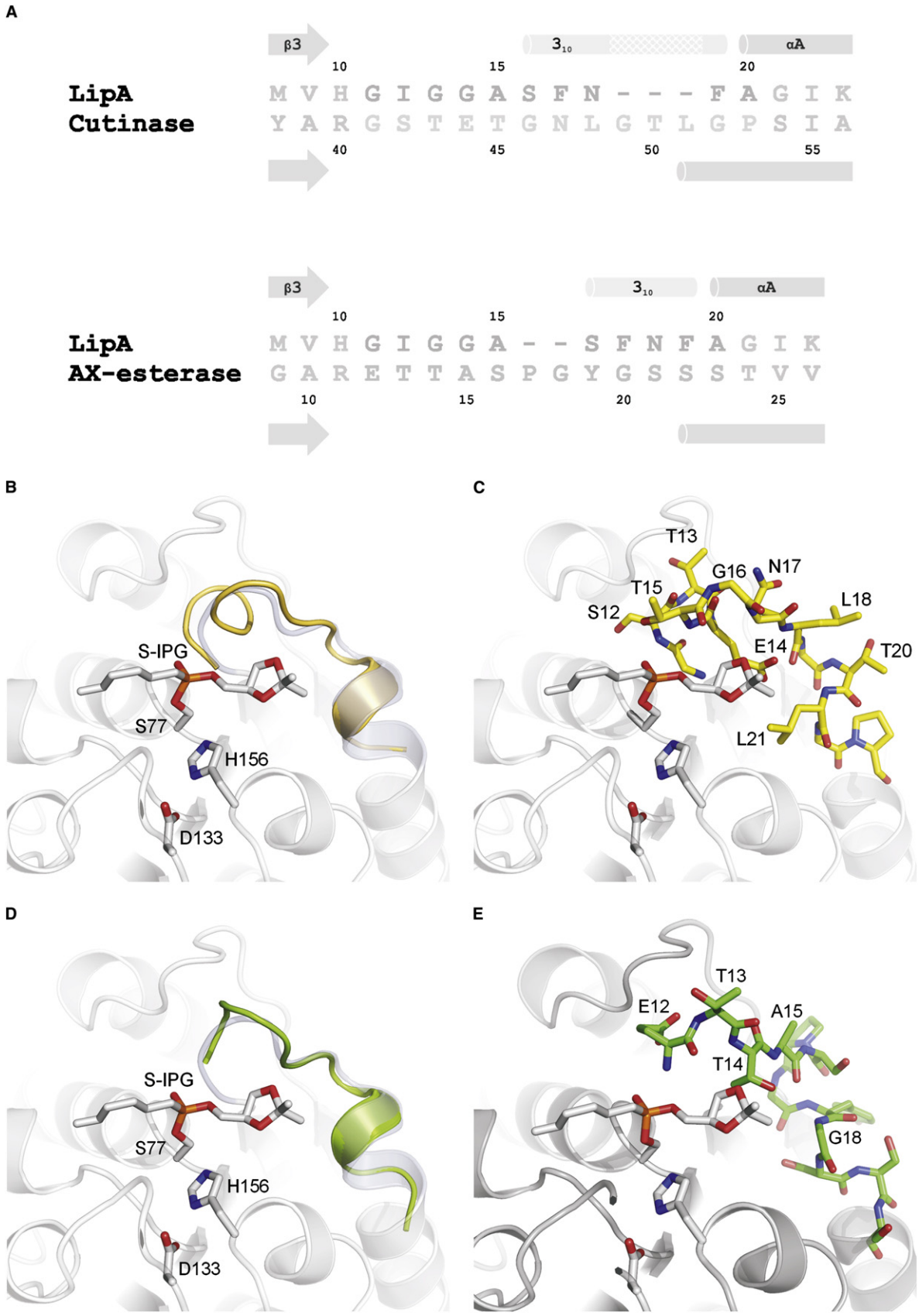
A
β3
3₁₀
αA
LipA
Cutinase
M V H G I G G A S F N - - - F A G I K
Y A R G S T E T G N L G T L G P S I A
10
15
20
40
45
50
55
β3
3₁₀
αA
LipA
AX-esterase
M V H G I G G A - - S F N F A G I K
G A R E T T A S P G Y G S S S T V V
10
15
20
25
B
S-IPG
S77
H156
D133
C
T13
G16
N17
T15
S12
L18
E14
T20
L21
D
S-IPG
S77
H156
D133
E
T13
E12
A15
T14
G18

loss in activity, from 22.4% to even 5.3% for variant T20K/L21G. In contrast to the first selection round on position L21, in this round the parent sequence T20T/L21G was selected for as well, although changes at the DNA level had occurred. For the L21Q parent, a loss in *ee* was observed, from +52.0% for L21Q itself to an *ee* value as low as +14.9% for the T20C/L21Q mutant. Selected variants showed activities similar to that of the L21Q parent.

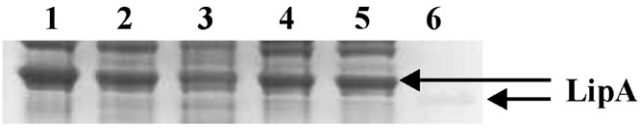

Figure 2. Expression of the Variants in the Periplasm of *E. coli* HB2151 on SDS-PAGE Gel

A total of 25 μg variant 1CEX (lane 2), 1CEX L21G (lane 4), and 1CEX L21Q (lane 5) was loaded. Wild-type LipA (lane 1) and an empty *E. coli* HB2151 strain (lane 3), as well as purified LipA (lane 6), were taken as a control. Note that the expressed proteins run slightly higher due to a His tag.

DISCUSSION

All lipases share the α/β-hydrolase fold, and most lipases have an α helix acting as a mobile lid controlling access to the active site. The lid region modulates not only the activity of the enzyme, but also its selectivity (Akoh et al., 2004; Brocca et al., 2003; Carrière et al., 1997; Dugi et al., 1995; Secundo et al., 2004; Seizaburo et al., 2005). Furthermore, mutations in the lid region can affect substrate preference and thermostability (Santarossa et al., 2005), and alterations of the enzyme's enantioselectivity have been described as well (Holmquist and Berglund, 1999). Thus, the role of the lid is more complicated than simply controlling access to the enzyme active site. In contrast, some lipases have been reported to have a solvent-exposed active site without a lid-like structure. An example of such a hydrolase is the *B. subtilis* LipA. In this study, we explored the feasibility of inserting somewhat longer loops near the active site in this enzyme. *F. solani* cutinase and *P. purpurogenum* acetylxylan esterase were previously identified as structural homologs to LipA (Van Pouderoyen et al., 2001). These enzymes feature the α/β-hydrolase fold as well, which enables rational mutagenesis and loop swapping. A loop near the active site was chosen for the exchange, as this loop has been indicated to be important for the enantioselectivity of the enzyme. Previously, position N18 within the wild-type loop was shown to affect enantioselectivity in such a way that enantiopreference was inverted toward the desired enantiomer of IPG, possibly by a better accommodation of the *S*-enantiomer in the active-site pocket of LipA (Dröge et al., 2006). Eggert et al. (2004) applied loop swapping to *B. subtilis* LipA as well. In contrast to the present study, they used the loop consisting of residues 39–51 of *B. subtilis* LipA, which is more remote from the active site. That loop was exchanged for loops from 1CEX (9 residues), AXE (10 residues), and human pancreatic lipase (25 residues). Instead of extending an active-site-lining loop, as presented in our work, it was hypothesized that the active site was now more shielded from the solvent. Their variants were enzymatically active on *p*-nitrophenyl palmitate or on tributyrin, although they had lower activity than the wild-type enzyme. A change in enantioselectivity was not determined. Based on our present work and that of Eggert et al. (2004), LipA appears to be compliant to loop swapping, in agreement with the versatile α/β-hydrolase scaffold that can accommodate many insertions and deletions (Nardini and Dijkstra, 1999).

The lack of a lid domain in LipA may explain its low enantiopreference toward the substrate of interest, IPG. Therefore, we assessed the effect of loop swapping/extension on the activity and the enantioselectivity of LipA in the conversion of racemic IPG butyrate. The constructed loop hybrids showed a conversion of IPG butyrate comparable to wild-type LipA. An inversion of the enantioselectivity was observed for both loop variants, although the K_M toward the desired enantiomer, *S*-(+)-IPG, was not significantly lowered. This indicates that the affinity of the enzyme for the desired substrate has not significantly changed.

The increased enantioselectivity might suggest that the desired enantiomer binds more productively. However, since ~7% of all LipA amino acids were altered, and since the changed amino acids are near the active site, we cannot exclude other explanations. The models suggest that the increased enantioselectivity may be due to an improved interacting surface with the *S*-enantiomer compared to the wild-type enzyme, since more residues are available for interaction with the substrate IPG. In the wild-type LipA, I12 functions in the stabilization of the transition state, being part of the preformed oxyanion hole. A15, F17, and N18 play a role in substrate binding. For the variant with the inserted AXE loop, the change in enantioselectivity was modest. Here, the nature of the binding pocket is most probably determined by E11, T12, A14, and S20, the residues closest to the IPG phosphonate inhibitor (Figures 1D and 1E). The active site might still be able to accommodate both enantiomers reasonably well, as hardly any enantiopreference is observed. For the cutinase loop variant, the change in enantioselectivity was more pronounced. This variant has three extra amino acid residues compared to the wild-type LipA, thereby possibly creating a more improved interaction surface for *S*-(+)-IPG. For this mutant, the residues closest to the IPG phosphonate inhibitor are S12, T13, N17, and L21 (Figures 1B and 1C). In addition, E14 and T15 may have an effect on the interaction with IPG.

Figure 1. Models of the Constructed Loop Variants Superimposed on LipA

(A) Alignment of LipA with cutinase and acetylxylan esterase in the region of residues 11–20, the region of loop replacement.

(B) Replacement of LipA residues 11–20 (light blue) with cutinase residues 41–53 (yellow); the phosphonate ester of *S*-(+)-IPG bound to LipA is shown in stick representation.

(C) Stick representation of the cutinase loop.

(D) Replacement of LipA residues 11–20 (light blue) with acetylxylan esterase residues 12–23 (green); the phosphonate ester of *S*-(+)-IPG bound to LipA is shown in stick representation.

(E) Stick representation of the acetylxylan esterase loop.

Table 1. Activity and Enantioselectivity of the Constructed Loop Mutants

Variant	Conversion (%)	*ee* (%)	Enantiomer Formed in Excess
WT LipA	28.2 ± 1.0	−12.9 ± 1.1	*R*-(−)-IPG
WT 1CEX	62.8 ± 6.1	+40.5 ± 2.4	*S*-(+)-IPG
1CEX	29.7 ± 1.0	+26.48 ± 1.6	*S*-(+)-IPG
AXE	20.9 ± 1.9	+6.0 ± 0.7	*S*-(+)-IPG

n = 3.

The cutinase variant proved to be more promising as a starting point for further optimization of the enantioselectivity by directed evolution (Bloom et al., 2005; Reetz, 2004). However, enantioselectivity being far from optimal, site-directed mutagenesis was applied to residue L21 in the exchanged loop region. This residue is at a position equivalent to N18 in the wild-type LipA, which previously has been shown to be important for the interaction with the substrate IPG (Dröge et al., 2006) and might therefore be important for the enzyme's enantioselectivity as well. Importantly, an improvement of enantioselectivity was observed for all selected variants. Mutants with a somewhat shorter side chain were favored in the selection. Indeed, mutant L21G was selected for six times. Additionally, the selected variants L21A and L21V showed high enantioselectivities as well. Due to their smaller side chains compared to leucine, a more compact folding might be possible. A glutamine residue was selected for three times; since it is a more polar residue and has a bigger side chain, more subtle changes will take place, leading to an improved enantioselectivity. The improved enantioselectivity suggests that residue L21 is indeed in interacting distance to IPG, thus corroborating the SWISS-MODEL-generated structure. Being in an equivalent position as N18 in the LipA wild-type, L21 thus also has an important influence on enantioselectivity. This observation might be substantiated by the fact that a similar improvement of the enantioselectivity was not observed when position T20 was mutated. Alhough these mutations resulted in somewhat less active variants, the enantioselectivity was equal to or less than the enantioselectivity of the respective parent loop mutant.

In conclusion, we have designed and engineered two lipase hybrids by exchanging stretches of amino acids. By changing a loop near the active site, lipase hybrids were created with inverted enantioselectivities compared to the wild-type parent enzyme. However, the inserted stretch of amino acids might not be the optimal sequence for the enzyme's enantioselectivity. Therefore, it would be worthwhile to optimize the enantioselectivity of this loop hybrid by randomizing the inserted loop region on these positions and assess which sequence is optimal. Consequently, we anticipate that the knowledge gained from this study will serve as a lead for future protein engineering to create lipases that are more enantioselective than those offered by nature.

Table 2. Determination of K_M Values

Enzyme	K_M (mM) Butyrate Ester of (−)-IPG	K_M (mM) Butyrate Ester of (+)-IPG
WT LipA	0.53 ± 0.33	1.05 ± 0.10
1CEX	1.00 ± 1.8	0.68 ± 0.53
1CEX L21G	1.17 ± 0.72	0.83 ± 0.11
1CEX L21Q	1.13 ± 3.2	0.52 ± 0.46

n = 3.

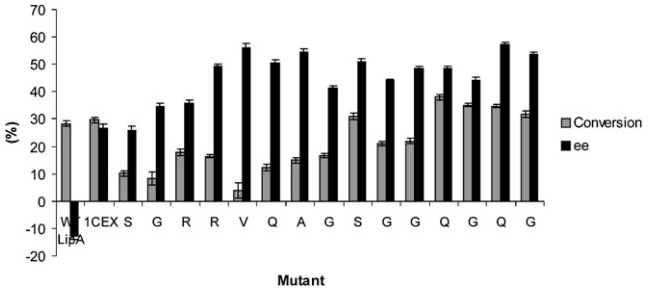

Figure 3. Activity and Enantioselectivity of Selected L21 Variants
n = 3.

SIGNIFICANCE

B. subtilis LipA has excellent properties with regard to its kinetics for application in industrial biocatalysis of enantiopure β-adrenergic receptor antagonists and, in particular, of their chiral building block 1,2-O-isopropylidene-_sn_-glycerol (IPG). Nevertheless, its enantioselectivity toward these substrates is modest, and, moreover, it is directed toward the unwanted enantiomer of IPG. From its crystal structure, it is known that LipA has a relatively open active-site cleft. It was previously demonstrated that a drastic change in amino acid sequence and active-site architecture can give rise to altered enzyme function. This implies the replacement of several of the enzyme's surface loop structures. Thus, we hypothesized that extending a loop lining the active-site cleft and consequently narrowing it, might improve and invert the enzyme's enantioselectivity. Homologs of LipA without a lid-like structure were identified, and the LipA hybrids were rationally designed. Exchange of loops from _F. solani_ cutinase and _P. purpurogenum_ acetylxylan esterase resulted in active LipA hybrids, which showed an inverted enantioselectivity. The enantioselectivity of the cutinase hybrid, being the more promising variant of the two, was further evolved by directed evolution. Thus, variants with

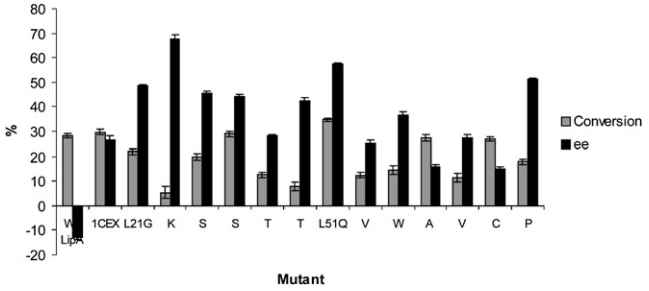

Figure 4. Activity and Enantioselectivity of Selection T20X/L21G and T20X/L21Q Double Mutants
T20X/L21G double mutants are shown on the left, and T20X/L21Q double mutants are shown on the right. n = 3.

improved enantioselectivity were selected by a growth-selection assay and were characterized.

From an engineering point of view, this work extends the use of enzyme engineering by grafting loops near the active site. The combination of rational design of the hybrids and directed evolution on specific hotspots has proven successful. Our work, therefore, provides novel, to our knowledge, perspectives on the evolution of enzyme enantioselectivity, and can lead to an application in the improved synthesis of enantiopure β-adrenergic receptor antagonists.

EXPERIMENTAL PROCEDURES

Computational Design of the Loop Mutants

B. subtilis LipA has an α/β-hydrolase fold that is very similar to that of cutinase from *F. solani* (Protein Data Bank entry 1CEX [Longhi et al., 1997]) and that of acetylxylan esterase (AXE) from *P. purpurogenum* (PDB entry 1G66 [Ghosh et al., 1999]) (Van Pouderoyen et al., 2001). The homology of the enzymes was calculated by using the SSM server (http://www.ebi.ac.uk/msd-srv/ssm [Krissinel and Henrick, 2005]). A superposition of LipA and cutinase structures showed that the 42–53 loop of cutinase is equivalent to residues 12–20 (Figure 1A). For AXE, residues 12–23 are equivalent to residues 11–20 in LipA (Figure 1A). By means of the SWISS-MODEL server, protein structure homology models were computed by using wild-type LipA as a template (PDB entry 1ISP) (http://swissmodel.expasy.org/workspace [Arnold et al., 2006]). Structure-based sequence alignments of the constructed models and LipA in the presence of the phosphonate ester of *S*-(+)-IPG (PDB code 1R50) were created with 3DCoffee (O'Sullivan et al., 2004). Modeler version 9.1 (Sali and Blundell, 1993), as implemented in the Biskit structural bioinformatics framework (Grunberg et al., 2007), was used to generate the resulting models (Figures 1B–1E).

Plasmids, Bacterial Strains, and Media

E. coli HB2151 (K12 Δ(*lac-pro*), *ara*, *nalr*, *thi*/F′, *pro*AB, *laq*Iq, *lac*ZΔ-M15) and pCANTAB 5E were purchased from Pharmacia (Amersham Pharmacia Biotech, Uppsala, Sweden). *E. coli* K-12 PA340/T6 (*thr-1, leuB6*(Am), *fhuA2*, *lacY1*, *glnV44*(AS), *gal-6*, λ^-, *gdhA1*, *hisG1*(Fs), *rfbD1*, *galP63*, Δ(*gltB-gltF*)*500*, *rpsL9*, *malT1*(λ^R), *xylA7*, *mtlA2*, Δ*argH1*, *thi-1*) was kindly provided by the *E. coli* Genetic Stock Center (Yale University, New Haven, CT). 2xTY medium contained: bactotrypton (1.6% w/v), bacto yeast extract (1% w/v), and sodium chloride (0.5% w/v). As antibiotic agents, ampicillin (100 μg.ml^{-1}), and streptomycin (100 μg.ml^{-1}) (Duchefa Biochemie, Haarlem, The Netherlands) were used. M8 minimal medium contained $Na_2HPO_4.7H_2O$ (4 g.l^{-1}), KH_2PO_4 (15 g.l^{-1}), and sodium chloride (2.5 g.l^{-1}).

Chemicals

Both enantiomers of aspartate esters of IPG as well as both enantiomers of butylphosphonate esters of IPG were synthesized by Syncom BV (Groningen, The Netherlands). Butyrate esters of both enantiomers of IPG were kindly provided by M.T. Reetz (Max-Planck Institut für Kohlenforschung, Mülheim, Germany). *p*-nitrophenyl caprylate was purchased from Sigma Chem. Co. (Axel, The Netherlands). Supplemental amino acids (Thr, Arg, Leu, His [10 mg.l^{-1}]) were purchased from Sigma-Aldrich (Steinheim, Germany).

Construction of the Loop Mutants

The LipA encoding gene (GenBank accession number M74010) was cloned in the phagemid pCANTAB 5E, downstream of a modified g3p signal sequence (Dröge et al., 2003b). To introduce the 1CEX 42–53 loop, an overlapping PCR strategy was used. All primers used in the reactions were purchased from Invitrogen (Groningen, The Netherlands) (for sequences, see Table S1 available online). In the first step, the 42–53 loop was constructed by using primer 1CEXfor in combination with LipAlooprev and primer 1CEXrev in combination with LipAloopfor. The AvaI restriction site, indicated in bold italics, was inserted to make restriction analysis possible. The two overlapping PCR "half fragments" were purified and used as a template in a second PCR step with the flanking primers LipAloopfor and LipAlooprev.

To construct the AXE mutant, the same PCR strategy was followed by using primer AXEfor in combination with LipAlooprev and primer AXErev in combination with LipAloopfor. The BamHI restriction site, indicated in bold italics, was put in to make restriction analysis possible. In a second PCR step, the obtained overlapping PCR fragments were combined by using LipAloopfor and LipAlooprev primers.

Mutant libraries on position 21 in the CEX loop were constructed by using primer 1CEXN51BamHIFor in combination with LipAlooprev and primer 1CEXN51BamHIRev in combination with LipAloopfor. The BamHI restriction site, indicated in bold italics, was put in to make restriction analysis possible. In a second PCR step, the obtained overlapping PCR fragments were combined by using LipAloopfor and LipAlooprev primers.

Mutant libraries on position 20 in the CEX loop with either a Gln (CAA) or a Gly (GGG) at position L21 (underlined) were constructed by using primer 1CEX5051XBamFor in combination with LipAlooprev and primer 1CEX5051X-BamRev in combination with LipAloopfor. The BamHI restriction site, indicated in bold italics, was put in to make restriction analysis possible. In a second PCR step, the obtained overlapping PCR fragments were combined by using LipAloopfor and LipAlooprev primers.

Recombinant DNA procedures were carried out as described by Sambrook et al. (1989). Plasmid DNA was prepared by using the Qiaprep Spin Miniprep kit (QIAGEN, Hilden, Germany). DNA purification was performed by using the Qiaquick Gel Extraction kit (QIAGEN, Hilden, Germany). The gene fragment was digested with AgeI and HindIII (New England Biolabs) and was cloned in *E. coli* HB2151 into the AgeI and HindIII sites of the phagemid pCANTABLip-CH (Dröge et al., 2003b). The constructs were sequenced to verify the correct base pair order.

Isolation of the Periplasmic Fraction

E. coli HB2151 or *E. coli* K-12 PA340/T6 were grown in 50 ml tubes containing 10 ml 2xTY medium, ampicillin, and isopropyl-β-d-galactopyranoside (IPTG, 1 mM). The tubes were incubated at 28°C at 250 rpm for 16 hr. The OD_{600} was recorded, and the cells were harvested and resuspended in Tris-HCl buffer (10 mM, pH 7.4). After centrifugation, the cells were resuspended in 200 μl buffer containing Tris-HCl (10 mM, pH 8.0), sucrose (25% w/v), EDTA (2 mM), and lysozyme (0.5 mg.ml^{-1}). After incubation on ice for 20 min, 50 μl buffer containing Tris-HCl (10 mM, pH 8.0), sucrose (20% w/v), and $MgCl_2$ (125 mM) was added. The suspension was centrifuged, and the supernatant, containing the periplasmic fraction, was isolated and used as enzyme solution in the IPG ester assay. The protein content of this fraction was determined by performing a Bradford assay in triplicate by using bovine serum albumin (BSA) as a standard (Pierce, Rockford, IL).

1,2-O-Isopropylidene-*sn*-Glycerol Ester Assay

Wild-type cutinase and periplasmic fractions were diluted with MOPS buffer (0.07 M, pH 7.5), containing BSA (0.2% w/v), to a final volume of 100 μl. References were diluted correspondingly but contained no enzyme solution. The esters of IPG (1 mM) were dissolved in 10 ml MOPS buffer (0.07 M, pH 7.5), containing Tween 80 (14.3% w/v), and were diluted to 50 ml with MOPS buffer (0.07 M, pH 7.5). A total of 500 μl substrate solution was added to the enzyme solution, and the final mixture was incubated in a water bath at 32°C. After incubation, 400 μl saturated NaCl solution and 10 μl internal standard solution (racemic 3-hexene-1-ol, 5 mg.ml^{-1} assay buffer) was added to the sample solution, and the aqueous solution was extracted twice with 1 ml ethyl acetate. GC analysis was performed as described by Dröge et al. (2003a). One unit (U) is defined as the amount of enzyme that hydrolyses 1 μmol IPG ester per minute. Enantiomeric excesses, *ee*, were calculated according to Chen et al. (1982) and were defined as the ability of the enzyme to distinguish between enantiomers. All data were expressed as mean ± SEM. The statistical significance of differences was tested at a significance level of $p < 0.05$ by using a two-tailed Student's t test.

Determination of K_M

E. coli HB2151 was grown for 16 hr at 37°C in 1 l 2xTY medium supplemented with 100 μg.ml^{-1} ampicillin and 1 mM IPTG. The periplasmic fraction was isolated as described above. The total protein content was determined by performing a Bradford assay with bovine serum albumin (BSA) as a standard (Pierce, Rockford, IL). To determine the expression level of LipA, parent mutant

1CEX and the variants L21G and L21Q, SDS-PAGE was performed on a 12% separating and a 3% stacking gel (Invitrogen, Groningen, The Netherlands). Molecular mass markers were purchased from Invitrogen.

To obtain a K_M value, the IPG assay was performed in triplicate. The K_M value for each enantiomer was obtained by fitting the experimental data from Eadie-Hofstee plots. The mean and SEM of three measurements were calculated.

Selection on Selective Minimal Medium

The aspartate auxotroph *E. coli* K-12 PA340/T6 was made chemically competent and transformed with 50 ng mutant plasmid DNA of the library at position L21 in the loop (Sambrook et al., 1989). Growth selection was performed as described by Boersma et al. (2008). Cells were starved by incubation in 0.9% NaCl for 2 hr at 37°C and were plated onto selective minimal medium agar plates supplemented with either aspartate or an ester of aspartate coupled to enantiopure IPG. To increase selection pressure, a phosphonate inhibitor, i.e., a phosphonate ester of enantiopure IPG, was added to the medium. After 2 days of growth, 16 colonies were randomly selected and sequenced. The periplasm was isolated, and activity and enantioselectivity were tested toward the real substrate, a racemic IPG butyrate ester.

As a second generation of LipA mutants, a saturated library was created at position T20 in the loop while L21 was mutated in either a glutamine or a glycine residue. Mutants were selected by using the growth-selection procedure as described above. Colonies were selected and sequenced. The periplasm was isolated, and activity was tested on racemic IPG butyrate.

SUPPLEMENTAL DATA

Supplemental Data include one table and can be found with the article online at http://www.chembiol.com/cgi/content/full/15/8/782/DC1/.

ACKNOWLEDGMENTS

This project was funded by the European Commission under project number QLK3-CT-2001-00519. We thank all of the partners for their discussions and contributions leading to the generation of this project, and M.R. Egmond for providing the cutinase wild-type enzyme. Y.L.B. would like to thank R.H. Cool for fruitful discussions.

Received: January 21, 2008
Revised: May 6, 2008
Accepted: June 6, 2008
Published: August 22, 2008

REFERENCES

Akoh, C.C., Lee, G.-C., and Shaw, J.-F. (2004). Protein engineering and applications of *Candida rugosa* lipase isoforms. Lipids *39*, 513–526.

Arnold, K., Bordoli, L., Kopp, J., and Schwede, T. (2006). The SWISS-MODEL workspace: a web-based environment for protein structure homology modelling. Bioinformatics *22*, 195–201.

Beisson, F., Tiss, A., Rivière, C., and Verger, R. (2000). Methods for lipase detection and assay: a critical review. Eur. J. Lipid Sci. Technol. *102*, 133–153.

Blaser, H.-U., Pugin, B., and Spindler, F. (2005). Progress in enantioselective catalysis assessed from an industrial point of view. J. Mol. Catal. Chem. *231*, 1–20.

Bloom, J.D., Meyer, M.M., Meinhold, P., Otey, C.R., MacMillan, D., and Arnold, F.H. (2005). Evolving strategies for enzyme engineering. Curr. Opin. Struct. Biol. *15*, 447–452.

Boersma, Y.L., Dröge, M.J., van der Sloot, A.M., Pijning, T., Cool, R.H., Dijkstra, B.W., and Quax, W.J. (2008). A novel selection system for enantioselectivity of *Bacillus subtilis* lipase A based on bacterial growth. ChemBioChem *9*, 1110–1115.

Breuer, M., Ditrich, K., Habicher, T., Hauer, B., Kesseler, M., Stürmer, R., and Zelinski, T. (2005). Industrial methods for the production of optically active intermediates. Angew. Chem. Int. Ed. Engl. *43*, 788–824.

Brocca, S., Secundo, F., Ossola, M., Alberghina, L., Carrea, G., and Lotti, M. (2003). Sequence of the lid affects activity and specificity of *Candida rugosa* lipase isoenzymes. Protein Sci. *12*, 2312–2319.

Carrière, F., Thirstrup, K., Hjorth, S., Ferrato, F., Nielsen, P.F., Withers-Martinez, C., Cambillau, C., Boel, E., Thim, L., and Verger, R. (1997). Pancreatic lipase structure-function relationships by domain exchange. Biochemistry *36*, 239–248.

Chen, C.S., Fujimoto, Y., Girdaukas, G., and Sih, C.J. (1982). Quantitative analyses of biochemical kinetic resolutions of enantiomers. J. Am. Chem. Soc. *109*, 7294–7299.

Dartois, V., Baulard, A., Schanck, K., and Colson, C. (1992). Cloning, nucleotide sequence and expression in *Escherichia coli* of a lipase gene from *Bacillus subtilis* 168. Biochim. Biophys. Acta *1131*, 253–260.

Dartois, V., Coppée, J.Y., Colson, C., and Baulard, A. (1994). Genetic analysis and overexpression of lipolytic activity in *Bacillus subtilis*. Appl. Environ. Microbiol. *60*, 1670–1673.

Dröge, M.J., Bos, R., Woerdenbag, H.J., and Quax, W.J. (2003a). Chiral gas chromatography for the determination of 1,2-O-isopropylidene-sn-glycerol stereoisomers. J. Sep. Sci. *26*, 1–6.

Dröge, M.J., Rüggeberg, C.J., van der Sloot, A.M., Schimmel, J., Dijkstra, D.S., Verhaert, R.M.D., Reetz, M.T., and Quax, W.J. (2003b). Binding of phage displayed *Bacillus subtilis* lipase A to a phosphonate suicide inhibitor. J. Biotechnol. *101*, 19–28.

Dröge, M.J., Boersma, Y.L., Van Pouderoyen, G., Vrenken, T.E., Rüggeberg, C.J., Reetz, M.T., Dijkstra, B.W., and Quax, W.J. (2006). Directed evolution of *Bacillus subtilis* Lipase A by use of enantiomeric phosphonate inhibitors: crystal structures and phage display selection. ChemBioChem *7*, 149–157.

Dugi, K.A., Dichek, H.L., and Santamarina-Fojo, S. (1995). Human hepatic and lipoprotein lipase: the loop covering the catalytic site mediates lipase substrate specificity. J. Biol. Chem. *270*, 25396–25401.

Eggert, T., Leggewie, C., Puls, M., Streit, W., Van Pouderoyen, G., Dijkstra, B.W., and Jaeger, K.-E. (2004). Novel biocatalysts by identification and design. Biocatal. Biotransform. *22*, 139–144.

Eggert, T., Funke, S.A., Rao, N.M., Acharya, P., Krumm, H., Reetz, M.T., and Jaeger, K.-E. (2005). Multiplex-PCR-based recombination as a novel high-fidelity method for directed evolution. ChemBioChem *6*, 1062–1067.

Ghosh, D., Erman, M., Sawicki, M., Lala, P., Weeks, D.R., Li, N., Pangborn, W., Thiel, D.J., Jörnvall, H., Gutierrez, R., and Eyzaguirre, J. (1999). Determination of a protein structure by iodination: the structure of iodinated acetylxylan esterase. Acta Crystallogr. D Biol. Crystallogr. *55*, 779–784.

Grunberg, R., Nilges, M., and Leckner, J. (2007). Biskit—a software platform for structural bioinformatics. Bioinformatics *23*, 769–770.

Holmquist, M. (2000). α/β hydrolase fold enzymes: structures, functions and mechanisms. Curr. Protein Pept. Sci. *1*, 209–235.

Holmquist, M., and Berglund, P. (1999). Creation of a synthetically useful lipase with higher than wild-type enantioselectivity and maintained catalytic activity. Org. Lett. *1*, 763–765.

Krissinel, E., and Henrick, K. (2005). Secondary-structure matching (SSM), a new tool for fast protein structure alignment in three dimensions. Acta Crystallogr. D Biol. Crystallogr. *60*, 2256–2268.

Lesuisse, E., Schanck, K., and Colson, C. (1993). Purification and preliminary characterization of the extracellular lipase of *Bacillus subtilis* 168, an extremely basic pH-tolerant enzyme. Eur. J. Biochem. *216*, 155–160.

Longhi, S., Czjzek, M., Lamzin, V., Nicolas, A., and Cambillau, C. (1997). Atomic resolution (1.0 Å) crystal structure of *Fusarium solani* cutinase: stereochemical analysis. J. Mol. Biol. *268*, 779–799.

Martinez, C., De Geus, P., Lauwereys, M., Matthyssens, M., and Cambillau, C. (1992). *Fusarium solani* cutinase is a lipolytic enzyme with a catalytic serine accessible to solvent. Nature *356*, 615–618.

Nardini, M., and Dijkstra, B.W. (1999). [α]/[β] Hydrolase fold enzymes: the family keeps growing. Curr. Opin. Struct. Biol. *9*, 732–737.

O'Sullivan, O., Suhre, K., Abergel, C., Higgins, D.G., and Notredame, C. (2004). 3DCoffee: combining protein sequences and structures within multiple sequence alignments. J. Mol. Biol. *340*, 385–395.

Reetz, M.T. (2004). Controlling the enantioselectivity of enzymes by directed evolution: practical and theoretical ramifications. Proc. Natl. Acad. Sci. USA *101*, 5716–5722.

Sali, A., and Blundell, T.L. (1993). Comparative protein modelling by satisfaction of spatial restraints. J. Mol. Biol. *234*, 779–815.

Sambrook, J., Fritsch, E.F., and Maniatis, T. (1989). Molecular Cloning: A Laboratory Manual (Cold Spring Harbor, NY: Cold Spring Harbor Laboratory Press).

Santarossa, G., Lafranconi, P.G., Alquati, C., DeGioia, L., Alberghina, L., Fantucci, P., and Lotti, M. (2005). Mutations in the "lid" region affect chain length specificity and thermostability of a *Pseudomonas fragi* lipase. FEBS Lett. *579*, 2383–2386.

Schmid, A., Dordick, J.S., Hauer, B., Kiener, A., Wubbolts, M., and Witholt, B. (2001). Industrial biocatalysis today and tomorrow. Nature *409*, 258–268.

Secundo, F., Carrea, G., Tarabiono, C., Brocca, S., and Lotti, M. (2004). Activity and enantioselectivity of wildtype and lid mutated *Candida rugosa* lipase isoform 1 in organic solvents. Biotechnol. Bioeng. *86*, 236–240.

Seizaburo, S., Masaji, I., Harukazu, F., Masahiro, N., and Mitsuyoshi, U. (2005). Creation of *Rhizopus oryzae* lipase having a unique oxyanion hole by combinatorial mutagenesis in the lid domain. Appl. Microbiol. Biotechnol. *68*, 779–785.

Van Pouderoyen, G., Eggert, T., Jaeger, K.-E., and Dijkstra, B.W. (2001). The crystal structure of *Bacillus subtilis* Lipase: a minimal α/β hydrolase fold enzyme. J. Mol. Biol. *309*, 215–226.

Verger, R. (1997). 'Interfacial activation' of lipases: facts and artifacts. Trends Biotechnol. *15*, 32–38.

Zhao, H., Chockalingam, K., and Chen, Z. (2002). Directed evolution of enzymes and pathways for industrial biocatalysis. Curr. Opin. Biotechnol. *13*, 104–110.